

Ordered clusters and dynamical states of particles in a vibrated fluid

Greg A. Voth¹, B. Bigger¹, M. R. Buckley¹, W. Losert^{1,2}, M. P. Brenner², H. A. Stone², and J. P. Gollub^{1,3}¹Department of Physics, Haverford College, Haverford PA 19041, U.S.A.²Division of Applied Sciences, Harvard University, Cambridge MA 02138, U.S.A³Department of Physics, University of Pennsylvania, Philadelphia PA 19104, U.S.A

Present address: IREAP, University of Maryland, College Park, MD 20742-3511

(March 22, 2024)

Fluid-mediated interactions between particles in a vibrating fluid lead to both long range attraction and short range repulsion. The resulting patterns include hexagonally ordered micro-crystallites, time-periodic structures, and chaotic fluctuating patterns with complex dynamics. A model based on streaming flow gives a good quantitative account of the attractive part of the interaction.

PACS: 45.70.Qj, 47.15.Cb, 05.65.+b

Many important systems consist of granular material flowing while immersed in fluid. In early experiments, Bagnold used fluid saturated granular flows to remove the effects of gravity [1]. Others have avoided interstitial fluid (even removing air) in order to observe pure granular behavior. However, the fluid can produce interactions between particles resulting in interesting macroscopic effects. For example, granular heaping due to fluid interactions has been investigated in vertically vibrated deep granular beds [2,3]. Also, a variety of interaction effects are important in sedimentation (for example [4]). Several systems show combinations of attractive and repulsive interactions which result in ordering of particles [5-8].

In this letter, we present experimental studies of novel phenomena that occur as a consequence of both attractive and repulsive interactions between non-brownian particles when they are vibrated in a fluid. The observations include clustering, ordered crystalline patterns, and dynamical fluctuating states. The fluid mediated interactions can be tuned to produce a striking variety of dynamical phenomena, and this provides an interesting new mechanism for self-assembly of ordered structures.

The attractive interaction can be understood quantitatively using a theory based on the mean streaming flow generated by the oscillating particles. A short-range repulsive interaction is also observed at large vibrational acceleration. This repulsion shows a very sharp onset as the acceleration is increased. Together the combination of attraction and repulsion results in particles being bound together without contact over a range of parameters. We demonstrate how these interactions allow micro-crystallites to form, for example hexagons surrounding a particle center. Small numbers of particles can form stable structures, while larger numbers of particles (> 7) move chaotically in a bound state with no long range order, a "mesoscopic liquid".

The experimental setup is shown in Fig. 1. We conduct all experiments in a rigid 6 cm diameter by 1.5 cm tall cylindrical aluminum container vibrated vertically by an electromagnetic vibrator. We completely fill the container with a water/glycerol mixture of kinematic

viscosity $\eta = 8$ cS (density $\rho = 1.15$ gm/cm³) and a sub-monolayer of uniform stainless steel spheres of diameter $d = 0.794$ mm and density 8.0 gm/cm³. A glass window seals the top of the cylinder to provide optical access and to avoid surface waves. The bottom plate is made of glass since its smoothness reduces random horizontal particle motion. We have used both flat glass and a concave lens for the bottom surface. The concave lens (focal length -1 m) makes no measurable change in the particle interactions; it is used to keep particles from slowly drifting to the edges of the cell due to imperfect leveling or slightly non-linear vibrational motion.

Both the frequency ($f = 2\pi$) and amplitude (M) of the vibration of the container are controlled externally. The nondimensional acceleration is given by $a = M/g$. The container oscillations cause the particles to vibrate vertically, typically contacting the cell bottom once each cycle. The particles remain within 1 or 2 particle diameters from the bottom over a wide range of accelerations. We image the entire system from above using a fast CCD camera. When the system is illuminated from an oblique angle, it is possible to measure the positions of the shadows of particles, and thereby to determine the amplitude of their vertical motion, A , defined as half the peak to peak displacement. The particle Reynolds number, $Re = \rho d A f = \eta$, ranges from 2 to 10.

In Fig. 2 we show the time evolution of an initially random distribution of particles. After the vibrator is started, the particles quickly collect into localized clusters, and the clusters then slowly coalesce in a manner reminiscent of coarsening in phase transitions.

A two particle system provides a particularly simple flow in which the particle attraction can be compared with theory. Figure 3 shows the distance between the centers of two particles as a function of time. The approach rate increases until they come into contact. The shape of these curves provides clear evidence that the clustering is due to a fluid-mediated interaction, and not to inelastic collisions, which cause clustering in a similar system with no fluid [9]. The separation also shows a small periodic modulation with the period of the vertical

vibration. Particles separate near their lowest point and approach near the highest point of their motion.

The attractive interaction can be quantified by considering the flow produced by each individual particle's motion. The vibrations produce an oscillatory flow around each particle, which is well approximated as a potential flow, outside of a boundary layer with approximate thickness $\delta_{osc} = \frac{a}{\sqrt{2}} = 1$. In the experiment at $f = 50$ Hz, $\delta_{osc} = 0.2$ mm, which is smaller than the particle radius, $a = 0.397$ mm. The potential flow near each oscillating particle is $u = r$, where $r = \frac{1}{2}A \sin(\omega t) a^3 \cos(\theta) = r^2$; here the origin is at the middle of the particle, and θ is the angle between a given location on the sphere and the forcing direction. At the particle surface, the component of the velocity field parallel to its surface is $u_{\theta}(\theta) = \frac{1}{2}A \sin(\omega t) \sin(\theta)$ [10].

Long ago Lord Rayleigh pointed out that when the magnitude of the oscillatory flow $u_{\theta} = u_{\theta}(\theta)$ varies along a solid surface, such as that of the particle, a steady secondary flow is generated [11,12]. For flow near the surface, mass conservation then requires that there is also a flow perpendicular to the boundary with magnitude $u_z = -\delta_{osc} \frac{\partial u_{\theta}}{\partial \theta}$. Since this flow is not entirely out of phase with u_{θ} in the boundary layer, every oscillation cycle transports a finite amount of momentum into the boundary layer. Hence there is a time independent force density on the fluid in the boundary layer, which is parallel to the boundary and of order $\rho \delta_{osc} \frac{\partial u_{\theta}}{\partial \theta}$, where ρ is the fluid density and δ_{osc} denotes time average over a cycle. This forcing produces a steady flow, which when balanced against the viscous force $\mu \nabla^2 u_{steady} = 0$ gives the magnitude of the steady flow at the edge of the oscillatory boundary layer $u_{steady} = \frac{\rho \delta_{osc}^2}{4\mu} \frac{\partial u_{\theta}}{\partial \theta}$.

Hence, a steady flow is produced with a magnitude $u_{steady} = \frac{\rho A^2}{4\mu} = a$. A careful analysis [13] shows that this steady flow pushes fluid away from the poles of each particle; and so there is a perpendicular flow velocity towards the equator. This steady flow is the origin of the attractive interactions between two particles.

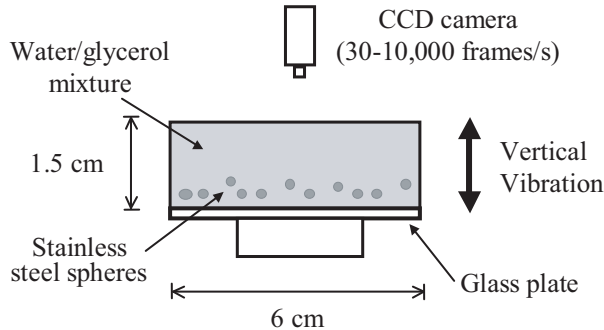


FIG. 1. Schematic of the apparatus in which particles are vibrated vertically in a viscous fluid. The vertical height of the cell is 19 times the particle diameter, so it approximates particles bouncing in a semi-infinite domain.

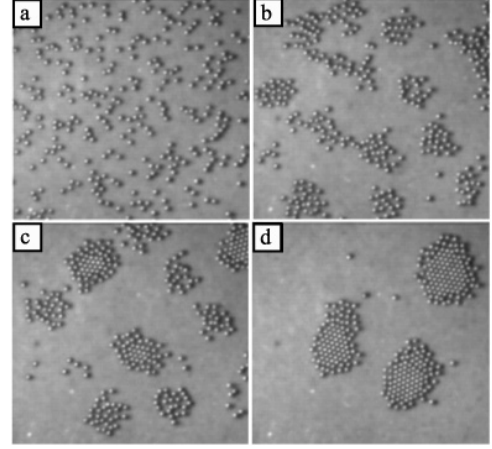


FIG. 2. Time evolution of an initially random distribution of beads. The attraction created by the streaming flow quickly collects the particles into clusters. ($f = 50$ Hz, $\omega = 4.5$) a) $t = 0$ s; b) $t = 8$ s, c) $t = 16$ s, d) $t = 32$ s.

To compute the rate at which particles come together, we must determine the in-flow velocity far from the particle. Besides the oscillatory boundary layer, there is also a boundary layer caused by the steady flow itself [14], with a scale $\delta_{steady} = a = \frac{a}{Re_{steady}}$, where $Re_{steady} = \frac{a u_{steady}}{\mu} = \frac{A^2}{2\mu}$ is the Reynolds number of the steady secondary flow. A matching argument, connecting the flows in the boundary layers to a potential flow far away, determines the in-flow velocity to be $v(r) = 0.53A \frac{\rho}{\mu} \frac{a^2}{r^3}$ at a distance r from the center of the sphere. Thus, if $R(t)$ denotes the distance between the particle centers, it follows that $dR/dt = -2v(R)$ since the particles follow the slow changes in the horizontal motion of the fluid. This implies that the separation between the two spheres should decrease according to the law

$$R(t) = (R_0^4 - 4.24A^2 \frac{\rho}{\mu} a^2 t)^{1/4} \quad (1)$$

This formula assumes that (i) $\delta_{osc} = \delta_{steady} < 1$, which can be rewritten $A < \frac{\mu}{\rho a^2}$; (ii) the particles are far enough apart that they do not affect each other's boundary layers; and (iii) neglects the influence of the bottom plate. Our estimates indicate that assumption (i) holds when a is small or f is large; (ii) holds except at the final moments of approach; and (iii) holds except during the small interval in each cycle when the particle bounces off the plate.

In Fig. 3, the central dashed line shows the approach curves predicted by Eq. 1 for the conditions of the experiment. The agreement of the data with both the predicted functional form and rate of approach is quite good considering that all the parameters used by the theory are independently determined. At 20 Hz (Fig. 3a), the measured trajectories approach somewhat more slowly than the theory predicts. At 50 Hz (Fig. 3b), the measured approach rate is closer to the prediction, and the functional

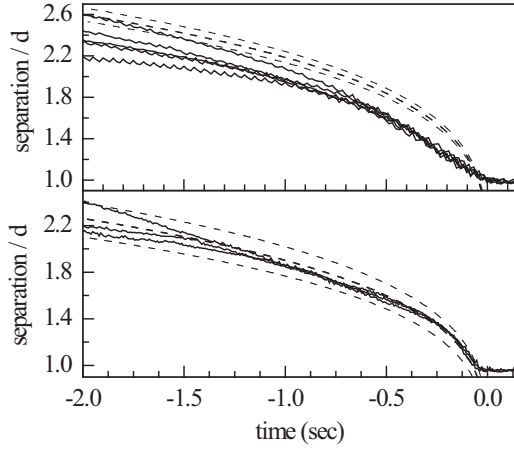


FIG. 3. Distance between two particles as they are brought together by the attractive flow. The solid curves are different experimental runs, and the central dashed curve shows the approach predicted by the steady streaming theory. Upper and lower dashed curves show the effect of measurement uncertainty in A . The time axes have been shifted so that the separation extrapolates to zero at $t = 0$. (a) $f = 20$ Hz, $\Gamma = 2.9$, $A = 0.41 \pm 0.04$ mm. Here the vertical particle motion is periodic. (b) $f = 50$ Hz, $\Gamma = 4.6$, $A = 0.15 \pm 0.04$ mm. The vertical motion is now chaotic and the mean oscillation amplitude is used for A in plotting the theoretical curve.

form agrees better, most likely because the oscillatory boundary layer is thinner in this case and so assumption (i) above is better satisfied. The upper and lower dashed curves show the effect of measurement uncertainty in A . Since at 50 Hz the amplitude is very small and the vertical motion is chaotic, the uncertainty is rather large in this case. Overall, the theory quite accurately captures the approach of two particles, and it seems unambiguous that the attraction is caused by the streaming mechanism.

At larger accelerations, a short-range repulsion becomes prominent and limits the closeness of approach. This can be seen in Fig. 4, which displays the steady state separation between two particles as a function of Γ for several different forcing frequencies. At each frequency, there is a step-like rise in separation at a characteristic Γ that moves to higher Γ as the frequency increases. It is interesting to note (Figure 4b) that there is no sharp change in the amplitude of the vertical motion of the particles with increasing Γ , so the onset of non-zero separation must be due to the fluid flow and not to changes in the bouncing dynamics. The onset of separation at each frequency appears when the particles have a peak-to-peak vertical amplitude of approximately 1.4d.

A fully quantitative theory of this effect is not available. One possible explanation is that the repulsion becomes important when the oscillatory boundary layer is thicker than the steady boundary layer. An alternate possibility suggested by flow visualization is that the re-

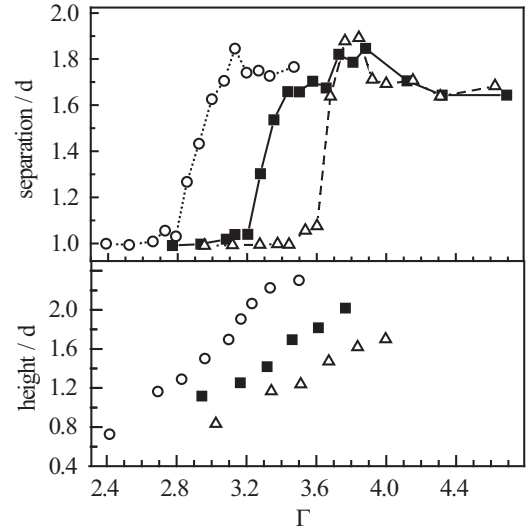


FIG. 4. (a) For two particles, the equilibrium distance between particle centers as a function of acceleration shows a rapid transition from contact to a nonzero separation. Separation is normalized by the particle diameter, d . (b) Measurements of the height that particles bounce above the plate show no dramatic change at the transition. Frequencies are 17 Hz (open circles), 20 Hz (filled squares), and 23 Hz (open triangles). Larger frequencies have the transition at larger acceleration.

pulsion is due to recirculating zones near the particles created by deflection of the downward part of the streaming flow by the plate. Explaining the details of the repulsive interaction remains as a challenge for future work.

Systems of more than two particles display a range of fascinating patterns and dynamics, including ordered crystallites, time-dependent ordered patterns, and bound states with complex particle motion. For example, one might expect that when attraction and repulsion are both important, the three particle system would form a stable symmetric triangular configuration. For low acceleration this is nearly the case, but as the acceleration increases, the system breaks symmetry to a state with two paired and one distant particle as shown in Fig. 5(a). This state is fairly stable, but over long times the distant particle can wander close enough to cause a new pairing.

In a system with 7 particles, stable hexagonal states form over the range $2.8 < \Gamma < 3.0$ (Fig. 5b). At slightly higher acceleration, the system switches to a time-dependent state with 2 central particles rotating inside a ring of 5 others (Fig. 5c). Particle motion here is periodic and quite stable, and an animation of this "dance" is available online [15]. At yet higher acceleration, 7 particle clusters exhibit apparently chaotic motion.

For larger numbers of particles, the presence of both attraction and repulsion leads to even more complex many body effects, which are generally time-dependent. Figures 5(d-f) show a system of many particles at 3 different

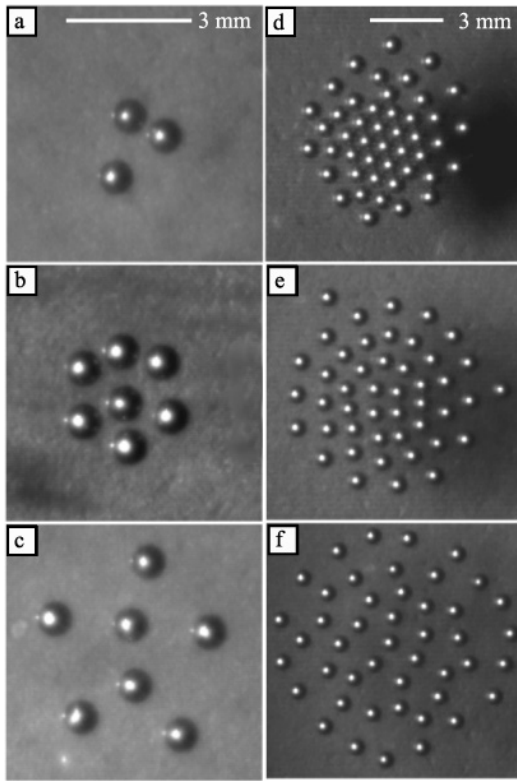


FIG. 5. Patterns formed by multiple particle systems when both attraction and repulsion are important. All images are acquired at $f = 20$ Hz. (a) 3 particles at $\Gamma = 3.0$. (b) 7 particles in a stable hexagon at $\Gamma = 3.0$. (c) 7 particles in stable time-periodic motion at $\Gamma = 3.7$. (d) Many particles at $\Gamma = 3.7$, where the central particles are in contact and exterior particles are held apart by the hydrodynamic repulsion. (e) At $\Gamma = 3.9$ all the particles have separated and form a bound liquid. (f) $\Gamma = 5.3$, apparently chaotic. The time-dependent character of states (c) through (f) are revealed in on-line animations [15].

accelerations. Here the onset of a non-zero separation between particles occurs at higher acceleration than for the two particle case. As shown in Fig. 5(d) ($\Gamma = 3.7$), particles near the center of the cluster can remain in contact even when particles near the periphery have separated. One reason for this is that the vertical motion of particles is significantly smaller at the center of the cluster than at the edges, causing weaker repulsion. At $\Gamma = 3.9$, (Fig 5e) the inner particles have separated and the system forms a bound state with weakly chaotic motion of all the particles, a "mesoscopic liquid". One interesting feature of this state is that the preferred distance between particles results in the formation of closed shells. At the parameters of Fig 5(e) there are two more particles than fit in the closed shells, and these "valence" particles move more freely than the others. Further increase of Γ results in increased interparticle distance and more rapid particle motion (Fig 5f). Animations of these time-dependent

states are available [15].

We emphasize that the chaotic motion of particles in the clusters is not a result of external effects such as roughness of the driving surface. A single particle bounces regularly with possibly a slow drift due to imperfect leveling or slightly non-vertical vibrator motion. Multiple particles exhibit complicated motion as a result of the nonlinearity of the flow of the interstitial fluid.

In summary, we have shown that fluid mediated interactions between particles can be delicately tuned to produce a great variety of ordered and time-dependent dynamical states of these many body systems.

This work has been supported in part by NSF grants DMR-0079909 to Haverford College, DMR-0072203 to The University of Pennsylvania, and DMS-0296056 to Harvard University. We appreciate the hospitality of the Aspen Center for Physics, where this collaboration began.

-
- [1] R.A. Bagnold, P. Roy. Soc. Lond. A Mat. 225, 49 (1954).
 - [2] H.K. Pak, E. Van Doo, and R.P. Behringer, Phys. Rev. Lett. 74, 4643 (1995).
 - [3] J.M. Schleier-Smith and H.A. Stone, Phys. Rev. Lett. 86, 3016 (2001).
 - [4] A.F. Fortes, D.D. Joseph, and R.S. Lundgren, J. Fluid Mech. 177, 467 (1987).
 - [5] M. Trau, D.A. Saville, and I.A. Aksay, Science 272, 706 (1996).
 - [6] S. Yeh, M. Seul, and B. Shraiman, Nature 386, 57 (1997).
 - [7] T. Gong and T.W. M. Marr, Langmuir 17, 2301 (2001).
 - [8] B.A. Grzybowski, H.A. Stone, and G.M. Whitesides, Nature 405, 1033 (1997).
 - [9] J.S. Olf and J.S. Urbach, Phys. Rev. Lett. 81, 4369 (1998).
 - [10] The flow field around each particle is modified by the presence of the bottom boundary; within the potential flow approximation having no mass flux across the plate requires an "image" particle beneath the plate, playing a similar role to image charges in electrostatics. Our estimates indicate that these image particles do not have a significant effect on the particle interactions.
 - [11] Lord Rayleigh, Philos. Trans. R. Soc. London Ser. A 175, 1 (1883).
 - [12] N. Riley, Annu. Rev. Fluid Mech 33, 43 (2001).
 - [13] N. Amin and N. Riley, J. Fluid Mech. 210, 459 (1990).
 - [14] Stuart, J.T. J. Fluid Mech. 24, 673 (1966).
 - [15] Animations are available at <http://www.haverford.edu/physics-astro/gollub/clustering/>